



Synthesis and characterization of mesoporous materials: Silica–zirconia and silica–titania

R.G. Rodríguez Avendaño^{a,b,*}, J.A. De Los Reyes^{a,b}, T. Viveros^{a,b}, J.A. Montoya De La Fuente^c

^a Universidad Autónoma Metropolitana, Departamento de Ingeniería de Procesos e Hidráulica, Av. Rafael Atlixco 186, Col. Vicentina, Iztapalapa, México, D.F., CP 09340, Mexico

^b Área de Ingeniería Química, Universidad Autónoma Metropolitana-Iztapalapa (UAM-I), México, D.F., CP 09340, D.F. Apodo. Postal 555-320-9000, Mexico

^c Instituto Mexicano del Petróleo, Dirección de Investigación y posgrado, Eje Central Lázaro Cárdenas 152, GAM, México, D.F., CP 07730, Mexico

ARTICLE INFO

Article history:

Available online 1 September 2009

Keywords:

Mesoporous
Sol–gel
Silica
Zirconia
Titania

ABSTRACT

An experimental strategy was developed to obtain mesoporous SiO₂–ZrO₂ and SiO₂–TiO₂ mixed oxides by a sol–gel method, treating the gels hydrothermally. The solids were characterized by nitrogen physisorption, pyridine thermodesorption, ²⁹Si nuclear magnetic resonance, SEM and X-ray diffraction. The effects of ZrO₂ content, the generated pressure in the synthesis vessel and further modification of this type of procedure on the solids properties were studied. It was found that SiO₂–ZrO₂ and SiO₂–TiO₂ mixed oxides dried at atmospheric pressure developed type I isotherms. On the other hand, for the SiO₂–ZrO₂ and SiO₂–TiO₂ mixed oxides that were treated under pressure in the autoclave (at high SiO₂ content) the porosity was improved and mesoporous materials exhibiting type IV adsorption isotherms. Specific surface area and pore size distribution were a function of ZrO₂ and TiO₂ content. The materials exhibited narrow pore size distributions with pore diameters in the region of mesopores at about 4 nm and high surface areas, the highest being 481 m²/g for the 10 wt% ZrO₂ Si–Zr material. Differences in acidity as determined by pyridine thermodesorption were observed to depend on the synthesis parameters and ZrO₂ and TiO₂ concentration.

© 2009 Elsevier B.V. All rights reserved.

1. Introduction

Silica is a naturally occurring material in minerals, such as quartz, and some plants such as bamboo, rice and barley. The properties of silica have been extensively studied by many authors, due to its wide range of applications [1,2]. Combinations of silica with a large number of other oxides have been reported [3]. On the other hand, oxides such as ZrO₂ and TiO₂ show very small specific surface area and low thermal stability, which reveal the importance to improve their textural properties or develop a new class of mesoporous materials [4]. In order to overcome these drawbacks, increasing attention has been paid to the development of mixed oxide supports by combining the higher surface areas and thermal stability of silica with the unique acidic properties of ZrO₂ and TiO₂. Mixed silica–titania and silica–zirconia materials are potentially useful in a number of technological applications, including catalysis of several reactions [5]. More particularly, previous work has been published on the silica–zirconia system as

synthesized by the sol–gel method [1,6]. SiO₂–ZrO₂ mixed oxides have gained increasing attention in recent years because of their interesting characteristics and many applications, which include alkali-durable glasses [7], catalyst support [8,9] and as an advanced ceramic material [10]. Comparison of the various results in the literature is sometimes difficult because of different preparation methods, sample treatments, or characterization techniques used to determine the structural and surface properties [11]. The representative method of preparation of porous materials in the SiO₂–ZrO₂ system is the sol–gel method [12], although the literature related to the synthesis of SiO₂–ZrO₂ is very scarce. The starting components are usually alcoholic solutions of alkoxides which undergo condensation reactions after initial hydrolysis. The homogeneous incorporation of Zr into a matrix is important to obtain materials that exhibit chemical, thermal and mechanical stabilities. The SiO₂–ZrO₂ and SiO₂–TiO₂ systems have been synthesized by different methods using surfactants for generating mesoporous materials [11]. Regarding textural and surface properties of various mixed oxides, the main attention in the literature has been paid to the influence of the complexing agents or surfactants used in the synthesis [2,17,18] and information about hydrothermal synthesis to obtain mesoporous silica–titania and silica–zirconia materials is scarce. Previous

* Corresponding author. Tel.: +52 55 5804 4800/83; fax: +52 55 5804 4876.

E-mail addresses: tvig@xanum.uam.mx, a_rgra@yahoo.com.mx

(R.G. Rodríguez Avendaño).

works in our group have pointed out the importance of a fine tuning of the synthesis conditions in order to produce solids with the desired characteristics [13–15]. The goal of the present work is to obtain mesoporous $\text{SiO}_2\text{--ZrO}_2$ and $\text{SiO}_2\text{--TiO}_2$ mixed oxides systems, based on a controlled hydrolysis-condensation process without using a surfactant as mesoporosity promoter. The experimental strategy developed allows the preparation of mesoporous materials when the gel is treated in an autoclave and heated to 423 K. Another important issue was to determine the acidic properties of $\text{SiO}_2\text{--ZrO}_2$ and $\text{SiO}_2\text{--TiO}_2$ systems [16]. We aim to provide a consistent picture in order to clarify structure-property relationships in silica-zirconia and silica-titania materials based on the combined results of different characterization techniques such as X-ray powder diffraction, N_2 physisorption, ^{29}Si NMR spectroscopy and FTIR pyridine thermodesorption.

2. Experimental

2.1. $\text{SiO}_2\text{--ZrO}_2$ synthesis

The materials were synthesized by a sol-gel modified method. As the SiO_2 and ZrO_2 sources, the chemical precursors used were tetraethylorthosilicate (TEOS) (Aldrich) and inorganic Zr-containing salt ($\text{Zr}(\text{NO}_3)_2$ (Aldrich), respectively. Nitric acid was used as hydrolysis catalyst. In a glass reactor, a proper amount of TEOS was dissolved in 300 ml of water at 358 K and then the acid catalyst was added. The mixture was maintained under vigorous stirring for 30 min and an aqueous solution of the Zr(IV) salt was added dropwise at 358 K to achieve $\text{ZrO}_2\text{:SiO}_2$ weight ratios of 0:100, 20:80, 40:60, 60:40 or 80:20. Stirring was continued for 120 min to promote hydrolysis and condensation. After condensation, the resulting gel was split into three fractions. The first fraction was dried at atmospheric pressure for 24 h. The second fraction was placed in an autoclave and heated at 423 K for 24 h. The third fraction was heated in an autoclave with water (20 g gel; 40 g H_2O) for 24 h at 423 K (hydrothermal synthesis). The resulting precursors were carefully dried and calcined in flowing air at 773 K. Samples were named in terms of the zirconium oxide concentration, i.e. Si-Zr (90 wt%–10 wt%) corresponds to a material containing 90 wt% SiO_2 and 10 wt% ZrO_2 , and so on.

2.2. $\text{SiO}_2\text{--TiO}_2$ synthesis

Titanium isopropoxide and tetraethylorthosilicate were used as sources of TiO_2 and SiO_2 , respectively. The synthesis recipe was as follows; TEOS was added to the nitric acid solution containing the proper amount of water at 358 K with magnetic stirring. After 25 min a clear solution was formed. Titanium isopropoxide was then added dropwise to the above solution under magnetic stirring for 30 min in order to form a sol. In sol-gel processes, domain formation due to the differences in the hydrolysis and the condensation rates of Ti and Si alkoxides was identified to be a major problem in the preparation of atomically mixed $\text{SiO}_2\text{--TiO}_2$ oxides. However, the two-stage hydrolysis procedure recently developed, which is performed in acidic conditions and using an appropriate alcohol solvent ($\text{C}_3\text{H}_8\text{O}$; isopropanol), seems to overcome this problem promoting suitable Ti–O–Si connectivity, which improves the cation homogeneity for the $\text{SiO}_2\text{--TiO}_2$ mixed oxides. The resulting gel was divided in three fractions and treated in a manner similar to that used in the $\text{SiO}_2\text{--ZrO}_2$ synthesis. The product was dried and calcined in air at 773 K for 2 h to obtain silica-titania mixed oxides. Samples were named in terms of the titanium oxide concentration, i.e. Si-Ti (90 wt%–10 wt%) corresponds to a material containing 90 wt% SiO_2 and 10 wt% TiO_2 .

2.3. Characterization

All the materials were characterized by XRD, N_2 physisorption, and their acid properties were analyzed by FTIR pyridine thermodesorption. The powder X-ray diffraction patterns were measured on a Siemens D-500 diffractometer with a graphite secondary beam monochromator, and the $\text{Cu K}\alpha_2$ contribution was eliminated by DIFFRAC/AT software ($\text{Cu K}\alpha_1$ radiation with $\lambda = 1.5406 \text{ \AA}$). Surface areas, pore size distributions, and pore volumes were measured by nitrogen adsorption at 77 K using Micromeritics Accusorb 2100 E equipment. The surface area was calculated with the BET method and the pore distribution with the Barrett-Joyner-Halenda (BJH) model. Before the analysis, the samples were treated at 573 K under vacuum. ^{29}Si NMR spectroscopy was performed with a high resolution solid-state spectrometer (Bruker, model 400) to study the changes in the SiO_2 structure when Zr(IV) species or Ti(IV) are incorporated into the silica network. ^{29}Si spectra were recorded at room temperature at a frequency of 79.4 MHz. Samples were spun at the magic angle using a frequency of 10 kHz. The pyridine adsorption was performed in a conventional flow adsorption system using N_2 as carrier (ratio; 2 l/h) for 30 min. The excess was eliminated with vacuum for 30 min. Afterward, the thermodesorption was made from room temperature to 773 K. The samples were analyzed in the range $1700\text{--}1400 \text{ cm}^{-1}$ (which has been assigned to the aromatic ring vibration in pyridine) using a PerkinElmer apparatus.

3. Results

3.1. N_2 Physisorption

3.1.1. $\text{SiO}_2\text{--ZrO}_2$ mixed oxides

N_2 adsorption-desorption isotherms for the silica-zirconia mixed oxides dried at room temperature (first fraction) are shown in Fig. 1. It was found that $\text{SiO}_2\text{--ZrO}_2$ mixed oxides develop type I isotherms [19], but the amount of N_2 adsorbed decreases as the ZrO_2 concentration increases. This result indicates that microporous materials were obtained with properties close to mesoporous materials and the ZrO_2 acts as a sintering material. The shallow hysteresis loop in the isotherm can be interpreted as the existence of narrow cylindrical pores [19].

On the other hand, the $\text{SiO}_2\text{--ZrO}_2$ gels that were treated in autoclave (at high SiO_2 content), second fraction exhibited type IV adsorption isotherms according to IUPAC classification, as seen in Fig. 2. It is observed that the low relative pressure point where the

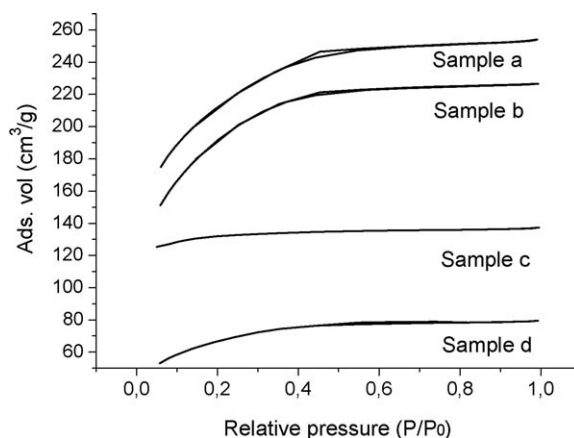


Fig. 1. Nitrogen adsorption-desorption isotherms for $\text{SiO}_2\text{--ZrO}_2$ mixed oxides with different ZrO_2 content. (a) Si-Zr (90 wt%–10 wt%), (b) Si-Zr (80 wt%–20 wt%), (c) Si-Zr (60 wt%–40 wt%), (d) Si-Zr (20 wt%–80 wt%), all the samples were dried at atmospheric pressure without autoclave.

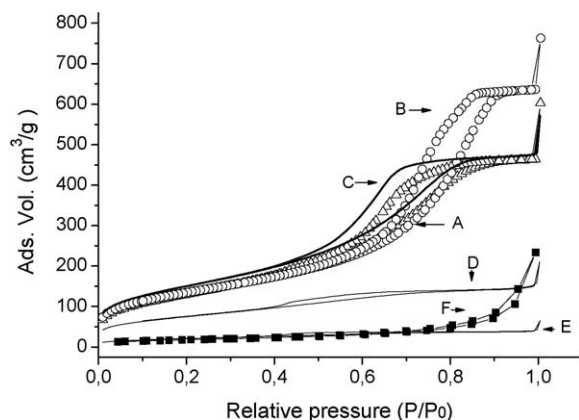


Fig. 2. Nitrogen adsorption-desorption isotherms for $\text{SiO}_2\text{-ZrO}_2$ mixed oxides with different ZrO_2 content. (A) Pure silica, (B) Si-Zr (90 wt%-10 wt%), (C) Si-Zr (80 wt%-20 wt%), (D) Si-Zr (40 wt%-60 wt%), (E) (20 wt%-80 wt%), (F) pure zirconia. All the samples were treated in autoclave and calcined at 773 K.

adsorption and desorption branches coincide, is affected by the ZrO_2 content of the sample. Hysteresis appears at higher relative pressures, indicating the occurrence of capillary condensation in larger pores (Fig. 2.). It can be observed that the second fraction with autoclave treatment is able to generate mesoporous $\text{SiO}_2\text{-ZrO}_2$ materials without the use of a surfactant. However, the appearance of mesoporous following the second fraction treatment depends on the ZrO_2 concentration. It is important to notice that the Si-Zr (90 wt%-10 wt%) sample develops a higher porosity than pure SiO_2 .

The pore size distribution of the mesoporous $\text{SiO}_2\text{-ZrO}_2$ materials is shown in Fig. 3. It was found that the pore size distribution is monomodal and narrow, for all mesoporous $\text{SiO}_2\text{-ZrO}_2$ materials. The SiO_2 , Si-Zr (90 wt%-10 wt%) and Si-Zr (80 wt%-20 wt%) show a pore diameter of about 4 nm and for the Si-Zr (90 wt%-10 wt%) and Si-Zr (80 wt%-20 wt%) the mean pore diameter diminishes to about 2 nm. The materials pore size structure shrinks as the ZrO_2 concentration increases in the mixed oxides.

The BET specific surface areas, pore volumes (V_p), average pore diameters for the $\text{SiO}_2\text{-ZrO}_2$ mixed oxides are given in Table 1. The results indicate surface areas depend on the ZrO_2 or TiO_2 concentration. It can be observed that large specific surface areas are obtained employing second fraction with autoclave treatment, being as high as $558 \text{ m}^2/\text{g}$ for the Si-Ti (95 wt%-5 wt%) sample. Samples with low concentration of SiO_2 (10 wt% SiO_2) shows small areas of around $60 \text{ m}^2/\text{g}$.

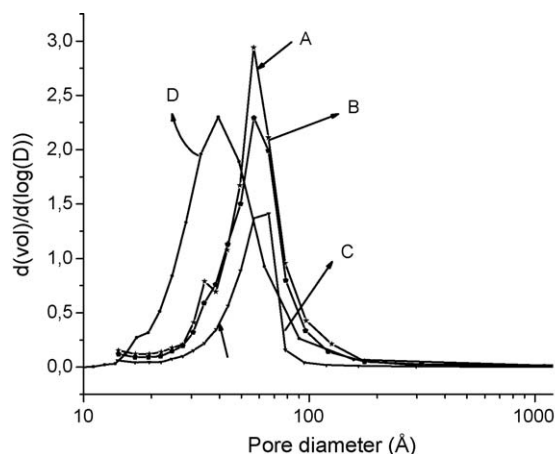


Fig. 3. Pore size distributions of $\text{SiO}_2\text{-ZrO}_2$ samples with different ZrO_2 content. (A) Pure silica, (B) Si-Zr (90 wt%-10 wt%), (C) Si-Zr (80 wt%-20 wt%), and (D) Si-Zr (40 wt%-60 wt%). All the samples were treated in autoclave and calcined at 773 K.

Table 1

Influence of the synthesis procedure on the texture. All samples treated in autoclave.

Sample	S_g^a (m^2/g)	ϕ_p^b (Å)	V_p^c (cm^3/g)
SiO_2	412	91	0.93
Si-Zr (90-10)	481	79	1
Si-Zr (80-20)	343	66	0.56
Si-Zr (40-60)	247	49	0.3
Si-Zr (20-80)	66	68	0.1
ZrO_2	50	25	0.35
Si-Ti (95-5)	558	71	0.9
Si-Ti (90-10)	484	60	0.7
Si-Ti (85-15)	434	73	0.79
Si-Ti (10-90)	58	70	0.11

^a Surface area.

^b Average pore diameter.

^c Pore volume.

Finally, $\text{SiO}_2\text{-ZrO}_2$ samples that underwent the hydrothermal treatment, heated in an autoclave with water (20 g gel; 40 g H_2O) for 24 h at 423 K (third fraction) exhibited type IV adsorption isotherms (at high SiO_2 content), following the same features as those observed for the second fraction materials. Hence, it was found that the concentration of water, does not affect the textural properties of the $\text{SiO}_2\text{-ZrO}_2$ materials.

3.1.2. $\text{SiO}_2\text{-TiO}_2$ mixed oxides

Fig. 4 shows N_2 adsorption-desorption isotherms for the $\text{SiO}_2\text{-TiO}_2$ mixed oxides. For all samples that were treated in the autoclave (second fraction) exhibit type IV isotherms at high silica content (Fig. 4), indicating that mesoporous materials had been obtained. When TiO_2 concentration increased from 5 wt% to 20 wt% the N_2 amount adsorbed diminished drastically. The increase of the adsorbed amounts at higher relative pressure is due to the increase of the mesopore volume (capillary condensation in mesopores).

Fig. 5 shows the pore size distribution (PSD) of the $\text{SiO}_2\text{-TiO}_2$ mixed oxides. PSDs are monomodal and broad and move toward larger pores when increasing the TiO_2 content in the samples.

3.2. X-ray diffraction

3.2.1. $\text{SiO}_2\text{-ZrO}_2$ mixed oxides

The diffraction patterns of SiO_2 , Si-Zr (80 wt%-20 wt%) and Si-Zr (60 wt%-40 wt%) mixed oxides are shown in Fig. 6. It was found that the materials were amorphous, suggesting that the ZrO_2 is

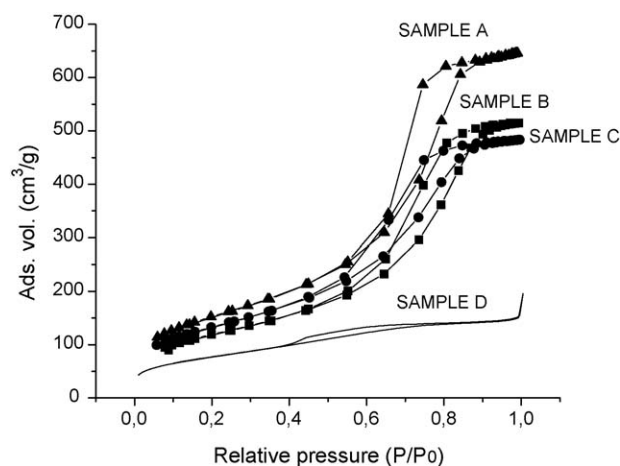


Fig. 4. Nitrogen adsorption-desorption isotherms for $\text{SiO}_2\text{-TiO}_2$ mixed oxides with different TiO_2 content. (A) Si-Ti (95 wt%-5 wt%), (B) Si-Ti (90 wt%-10 wt%), (C) Si-Ti (80 wt%-20 wt%), (D) Si-Ti (10 wt%-90 wt%). All the samples were treated in autoclave and calcined at 773 K.

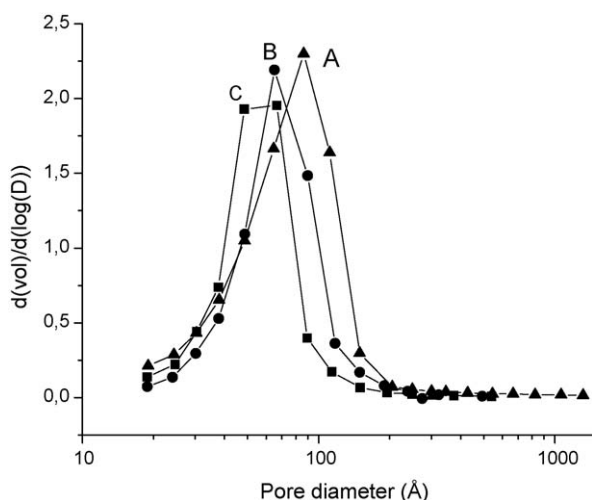


Fig. 5. Pore size distributions of $\text{SiO}_2\text{-TiO}_2$ mixed oxides with different TiO_2 content. (A) Si-Ti (95 wt%–5 wt%), (B) Si-Ti (85 wt%–15 wt%), (C) Si-Ti (90 wt%–10 wt%). All samples were treated in autoclave and calcined at 773 K.

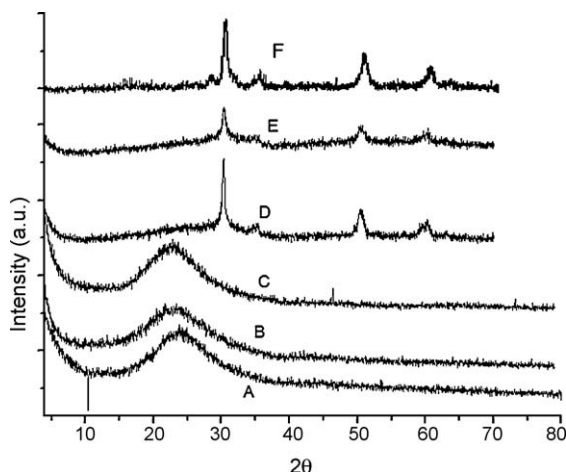


Fig. 6. XRD patterns of $\text{SiO}_2\text{-ZrO}_2$ with different ZrO_2 content. (A) Pure silica, (B) Si-Zr (90 wt%–10 wt%), and (C) Si-Zr (80 wt%–20 wt%), (D) Si-Zr (60 wt%–40 wt%), (E) Si-Zr (20 wt%–80 wt%), (F) Pure zirconia. All samples were treated in autoclave and calcined at 773 K.

highly dispersed into the SiO_2 matrix. In comparison, for the silica–zirconia mixed oxides at lower SiO_2 content, samples Si-Zr (40 wt%–60 wt%) and Si-Zr (20 wt%–80 wt%), extensive crystallization of ZrO_2 occur. The ZrO_2 crystallized in a mixture of tetragonal and cubic phases. The increase of intensity of the reflections is due to increment of the ZrO_2 crystallized. The incorporation of Zr into the framework of SiO_2 at molecular scale can be considered in the high SiO_2 content materials.

Usually there is a limit for mixing two oxides, beyond which segregation occurs. Under the present sol–gel synthesis conditions, the maximum miscibility of ZrO_2 and SiO_2 falls on the range of ca. 40 wt% of ZrO_2 . In other words structural and textural properties were the same for pure silica and silica–zirconia mixed oxides at Zr content <40 wt%.

3.2.2. $\text{SiO}_2\text{-TiO}_2$ mixed oxides

X-ray diffraction patterns were obtained for the calcined samples at several TiO_2 contents (with titanium isopropoxide as the TiO_2 precursor). Fig. 7 shows the amorphous diffraction patterns obtained for samples with high SiO_2 content (pure silica, Si-Ti (99 wt%–1 wt%), Si-Ti (95 wt%–5 wt%), Si-Ti (90 wt%–10 wt%), Si-Ti (85 wt%–15 wt%)) all the samples treated in

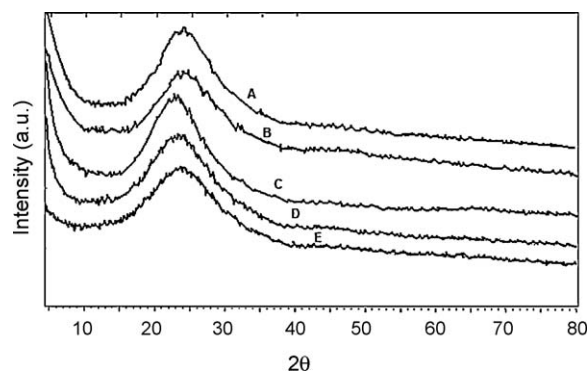


Fig. 7. XRD patterns of porous $\text{SiO}_2\text{-TiO}_2$ with different TiO_2 content. (A) Pure silica, (B) Si-Ti (99 wt%–1 wt%), (C) Si-Ti (95 wt%–5 wt%), (D) Si-Ti (90 wt%–10 wt%), (E) Si-Ti (85 wt%–15 wt%). All samples treated in autoclave and calcined at 773 K.

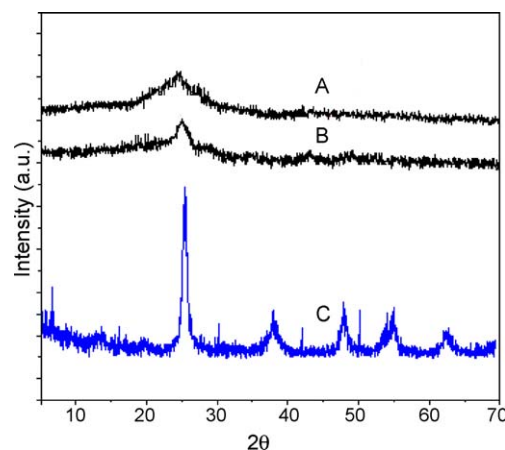


Fig. 8. XRD patterns of $\text{SiO}_2\text{-TiO}_2$ with high TiO_2 content (A) Si-Ti (60 wt%–40 wt%), (B) Si-Ti (20 wt%–80 wt%), (C) Pure titania. All samples treated in autoclave and calcined at 773 K.

autoclave (second fraction) and calcined at 773 K, whereas those corresponding to the samples dried in an autoclave at high TiO_2 content were crystalline, showing the presence of anatase TiO_2 crystalline phase (see Fig. 8).

In particular, crystallization was observed in samples Si-Ti (60 wt%–40 wt%) and Si-Ti (40 wt%–60 wt%), and a comparison of the peak intensities in Fig. 8 suggests that increasing TiO_2 content in the mixed oxides leads to a corresponding increase in the abundance of crystalline phase. For the samples with high TiO_2 content it is interesting to note that no other phases were observed. The atomically mixed $\text{SiO}_2\text{-TiO}_2$ oxides can only be obtained at low TiO_2 content, with the maximum TiO_2 solubility concentration lower than 15 wt% or Si/Ti atomic ratio higher than 7.5. At higher Ti contents, TiO_2 crystallites tend to form as a separate phase, demonstrating that silica could not favorably accommodate all the Ti atoms in the network above a certain limit. Increasing the concentration of TiO_2 above 15 wt% crystalline TiO_2 aggregates were found as a second phase at ca. 40 wt% TiO_2 .

3.3. ^{29}Si NMR spectroscopy

3.3.1. $\text{SiO}_2\text{-ZrO}_2$ mixed oxides

Experiments were performed with a high resolution solid-state NMR spectrometer (Bruker, model 400). ^{29}Si is a powerful technique for investigating the local environment of Si(IV) sites in materials such as $\text{SiO}_2\text{-ZrO}_2$ and $\text{SiO}_2\text{-TiO}_2$. ^{29}Si shows chemical shift for the observable resonances of the silica. The experimental

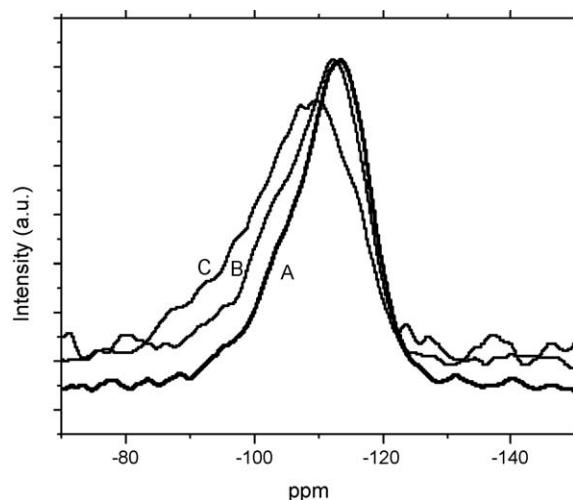


Fig. 9. ^{29}Si NMR of $\text{SiO}_2\text{-ZrO}_2$ with different ZrO_2 content. (A) Si-Zr (90 wt%–10 wt%), (B) Si-Zr (80 wt%–20 wt%), and (C) Si-Zr (20 wt%–80 wt%). All the samples were treated in autoclave and calcined at 773 K.

results of ^{29}Si for the $\text{SiO}_2\text{-ZrO}_2$ samples are shown in Fig. 9. The $\text{SiO}_2\text{-ZrO}_2$ samples with high silica content resonance corresponds to species with three siloxane bonds and one hydroxyl group (silanol sites), as the content of the second metal (Zr) is increasing, the resonance corresponds to silicon atoms with four siloxane attachments (interconnecting lattice sites), and resonance due to silicon atoms with two siloxane bonds and two hydroxyls (silanediol sites).

Samples Si-Zr (90 wt%–10 wt%) and Si-Zr (80 wt%–20 wt%) exhibit resonances near -100 and -110 ppm, attributed to Q^3 (Si(IV) with three siloxane bonds and one hydroxyl group) and Q^4 sites, respectively (Si(IV) with four siloxane bonds—interconnecting lattice sites) (Fig. 9(A) and (B)). Increasing Zr(IV) content (Fig. 9(C)), leads to the appearance of an additional peak near -90 ppm, assigned to Q^2 sites (Si(IV) with two siloxane bonds and two hydroxyls). The Q^4 Silicon atoms are dominant in pure silica, indicating that the silica has a well developed three-dimensional framework. The amounts of Q^3 and Q^2 increase with increasing Zr content. However, the comparison of $-\text{OH}$ and $-\text{OZr}$ groups is difficult because they have a similar influence on the chemical shift of the central Si atoms.

The presence of strong Si(IV)–Zr(IV) interactions in $\text{SiO}_2\text{-ZrO}_2$ mixed oxides can be indirectly inferred from the ^{29}Si NMR spectroscopy and XRD. From these data, two types of Zr(IV) species are present: (1) segregated ZrO_2 microdomains observed at relatively high Zr(IV) contents, which give rise to the characteristic diffraction peaks observed in Fig. 6, and which are associated with the presence of the Q^2 sites observed in Fig. 9(C); (2) isolated (amorphous) Zr(IV) species, observed at relatively low Zr(IV) contents. The relative abundance of these species is controlled by the chemical composition, the preparation methods, synthesis conditions (the hydrolysis route, Zr content, drying method and calcination temperature).

3.3.2. $\text{SiO}_2\text{-TiO}_2$ mixed oxides

In $\text{SiO}_2\text{-TiO}_2$ mixed oxides the degree of homogeneity at the atomic level is commonly associated with the relative amount of Si–O–Ti linkages in $\text{SiO}_2\text{-TiO}_2$ mixed oxides, and Si–O–Ti bonds are more effectively formed as the homogeneity increase. However, this technique cannot provide quantitative information about the Ti–O–Si linkages because the ^{29}Si resonances from Si–O–H and Si–O–Ti bonds are not distinguishable. In addition, this technique is not sensitive to the presence of crystalline TiO_2 (Fig. 10).

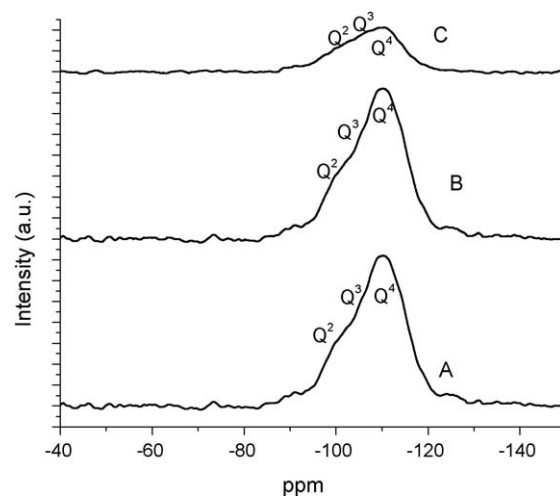


Fig. 10. ^{29}Si NMR of $\text{SiO}_2\text{-TiO}_2$ with different TiO_2 content. (A) Si-Ti (95 wt%–5 wt%), (B) Si-Ti (90 wt%–10 wt%), (C) Si-Ti (85 wt%–15 wt%). All the samples were treated in autoclave and calcined at 773 K.

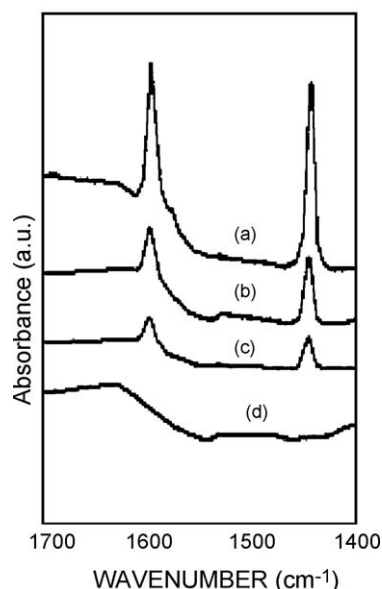


Fig. 11. Pyridine thermodesorption on pure SiO_2 treated in autoclave and calcined at 773 K. (a) Room temperature, (b) 373 K, (c) 473 K, (d) 573 K.

3.4. Pyridine thermodesorption

3.4.1. $\text{SiO}_2\text{-ZrO}_2$ mixed oxides

The acid properties of silica–zirconia are quite different from that of either pure zirconia or pure silica. SiO_2 is known to show little acidity, adsorbing only small amounts of pyridine which are easily removed. The observed bands (1597 and 1446 cm^{-1}) in Fig. 11 are typical of hydrogen bonded interactions, i.e. OH groups which are not acidic enough to transfer their proton to pyridine. Only pyridine hydrogen bonded to the silica surface is present. On adsorption at room temperature Fig. 11(a) bands attributed to physisorbed pyridine (weakly bound to the surface) are observed.

The adsorption of pyridine on the mixed oxides was performed to obtain the acidity of the surface. $\text{SiO}_2\text{-ZrO}_2$ and $\text{SiO}_2\text{-TiO}_2$ mixed oxides not only possess Lewis acidity but also generate Brønsted acid sites. The location of these Zr or Ti atoms should be on the surface of micro-, meso- or macro-pores that are accessible to the reactants or probe molecules. Fig. 12 shows the spectra of pyridine

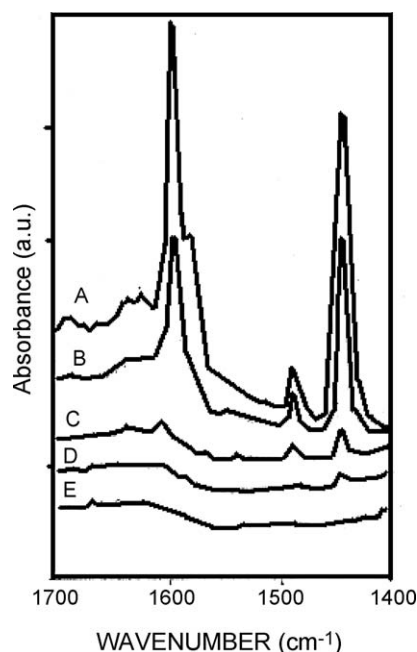


Fig. 12. Pyridine thermodesorption on $\text{SiO}_2\text{-ZrO}_2$ (90 wt%-10 wt%), the sample was treated in autoclave and calcined at 773 K. (A) Room temperature, (B) 373 K, (C) 473 K, (D) 573 K, (E) 673 K.

at different temperatures in the range 298–673 K for the sample Si-Zr (90 wt%-10 wt%). It is observed that bands corresponding to Lewis sites are stronger and more abundant than those of Brønsted sites, therefore the amount of Lewis acid sites is much higher than the Brønsted acid sites and they remain until 673 K, indicating they are strong acid sites. In comparison, the same sample Si-Zr (90 wt%-10 wt%) (Fig. 13) obtained by hydrothermal treatment with water, Brønsted acid sites are almost non-existent, and the total acidity (Lewis and Brønsted) is eliminated at low temperatures, having a strength which is lower than the Si-Zr (90 wt%-10 wt%) coming from the second fraction. This result indicates that not only the mesoporous structure is modified by the hydrothermal synthesis but also the acidity, which is associated with the distribution and interaction of the second cation.

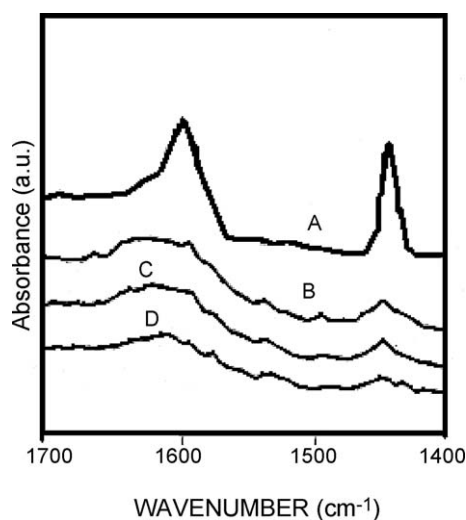


Fig. 13. Pyridine thermodesorption on $\text{SiO}_2\text{-ZrO}_2$ (90 wt%-10 wt%), the sample was treated in autoclave with water (hydrothermal synthesis) and calcined at 773 K. (A) Room temperature, (B) 373 K, (C) 473 K, (D) 573 K.

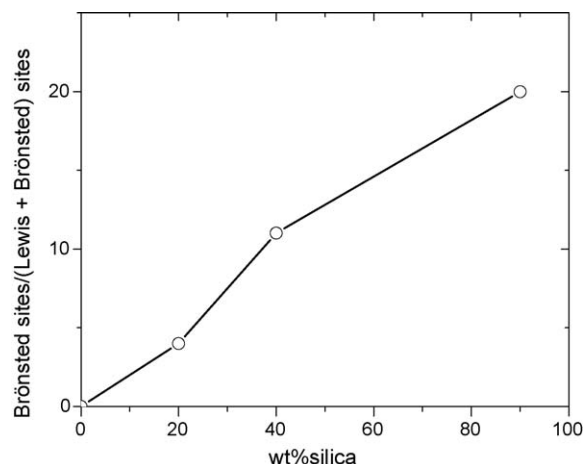


Fig. 14. Fractional Brønsted population, defined as Brønsted sites/[Lewis sites + Brønsted sites], as a function of composition for the $\text{SiO}_2\text{-ZrO}_2$ samples. All samples were treated in autoclave and calcined at 773 K.

These results indicate that the distribution of surface sites is modulated by the environment within the autoclave, with the second fraction yielding both Brønsted and Lewis acidity, whereas the Brønsted acidity is suppressed by hydrothermal processing when water is used. The results on this system (Si-Zr) could be explained in terms of the structural modifications that the inclusion of ZrO_2 brings about. With a mixed oxide material, surface acidic sites are formed due to the difference of the electronegativity between the two cations. According to the acidity hypothesis of the mixed oxides, the amount of the solid acid should be proportional to the number of Zr-O-Si and Ti-O-Si bonds. It appears that the formation of hetero-linkages of Zr-O-Si and Ti-O-Si produces higher acidity in the samples. Fig. 14 shows the relationship of ZrO_2 concentration and the relative Brønsted acidity of the samples. It is interesting to note that the highest Brønsted acidity is obtained with the Si-Zr (90 wt%-10 wt%) sample.

4. Discussion

The results presented in this work show that employing the sol-gel method for the synthesis of mixed oxides of $\text{SiO}_2\text{-ZrO}_2$ and $\text{SiO}_2\text{-TiO}_2$ followed by a solvothermal treatment under pressure it is possible to obtain mesoporous materials with interesting textural and surface properties. Surface areas, pore volumes, and average pore diameters of the samples calcined at 773 K are high, a function of the ZrO_2 or TiO_2 content and the higher surface areas are obtained at low concentrations of the promoter. More interesting is the fact that samples without the pressure treatment show no hysteresis in the adsorption-desorption isotherm, indicating the absence of pores in the mesoporous size; whereas those that underwent the treatment, developed characteristics of mesoporous materials.

The incorporation of ZrO_2 or TiO_2 at relatively low concentrations produce X-ray amorphous materials, and as the concentration increases reflections typical of the ZrO_2 or TiO_2 appear (Figs. 6–8). The spectra of crystalline pure ZrO_2 and TiO_2 are shown for comparison. These results indicate that a crystalline phase was present and segregated.

The amorphous characteristic of the mixed oxides at low concentration of TiO_2 or ZrO_2 suggest the possibility of formation of new Si-O-Zr and Si-O-Ti bonds in the mixed $\text{SiO}_2\text{-ZrO}_2$ and $\text{SiO}_2\text{-TiO}_2$ oxides. NMR results give information regarding this issue. Fig. 10 shows the ^{29}Si single-pulse (SP) solid-state MAS NMR spectra for the silica-titania mixed oxides with different titania

content. The SP SiO₂ spectrum exhibits three Gaussian peaks at chemical shifts, which can be assigned to Q⁴[Si(SiO)₄], Q³[Si(SiO)₃(OH)], and Q²[Si(SiO)₂(OH)₂] structural units, respectively. Q⁴ sites are dominant in pure silica, indicating a well developed three dimensional framework, however, the relative amount of Q⁴ sites decreases as the amount of titania increases. Some Si atoms were replaced by Ti atoms, indicating that Si–O–Ti bonds were generated upon the chemical mixing.

The acidity of silica–zirconia samples depends also on the zirconia concentration, and the highest acidity was found at the highest silica content tested (Si–Zr (90 wt%–10 wt%)). The absolute range of acidity is higher in silica–zirconia than silica–titania, and these differences can be related to the type and number of hetero-linkages (M–O–Si; M = Ti, Zr) formed in the two systems, in agreement with the Tanabe model [16]. The substitution of silicon by zirconium or titanium will result, in consequence, in the creation of one positive charge on the surface. Positive excess charge, which is presumably balanced by negative charges distributed elsewhere in the mixed oxide matrix, is associated with a Lewis site. The application of the Tanabe model to silica–zirconia and silica–titania predicts a preference for Lewis sites in the zirconia-rich and titania-rich region and Brønsted sites at silica-rich compositions. The partial positive charge in a mixed oxide catalyst can be explained as surface acidic sites formed due to the difference in electronegativity between the two cations Si–Zr, and Si–Ti. According to the acidity hypothesis of the mixed oxides, the amount of the solid acid should be proportional to the number of Zr–O–Si and Ti–O–Si bonds. However, a complete and detailed study of this model is required. One important point that should be mentioned is the fact that samples treated under pressure and with water added as a solvent, the mesoporous materials obtained did not show acidity, in clear contrast with those pressure treated without water.

5. Conclusions

SiO₂–ZrO₂ and SiO₂–TiO₂ have been prepared by the sol–gel method. The results reported in this work clearly indicate that sol–gel methods can be a viable way to prepare mesoporous SiO₂–ZrO₂

and SiO₂–TiO₂ mixed oxides. The materials exhibited pore diameters in the region of mesopores and high surface areas when the gel was treated in an autoclave (second fraction). It was found that the ZrO₂ or TiO₂ content influences the texture, structure and morphology of the samples. The textural properties were basically the same for the second fraction with autoclave and hydrothermal synthesis; however, differences in acidity were obtained depending on the treatment followed.

Acknowledgements

The authors wish to thank CONACYT, for its financial support. R.G. Rodríguez thanks CONACYT also for the scholarship.

References

- [1] J.A. Navio, M. Macias, G. Colón, J.M. Marinas, *J. Catal.* 161 (1996) 605.
- [2] Q. Zhuang, J.M. Miller, *Appl. Catal. A: Gen.* 209 (2001) L1.
- [3] B.M. Reddy, B. Chowdhury, P.G. Swirniotis, *Appl. Catal. A: Gen.* 211 (2001) 19.
- [4] V.I. Parvulescu, V. Parvulescu, U. Endruschat, Ch.W. Lehmann, P. Grange, G. Poncelet, H. Bönnemann, *Microporous Mater.* 44–45 (2001) 221.
- [5] A.O. Bianchi, M. Campanati, P. Maireles-Torres, E. Rodríguez Castellon, A. Jimenez López, A. Vaccari, *Appl. Catal. A: Gen.* 220 (2001) 105.
- [6] M. Aizawa, Y. Nosaka, N. Fujii, *J. Non-Cryst. Sol.* 128 (1991) 77.
- [7] F. Gonella, G. Matter, P. Mazzoldi, *Chem. Mater.* 11 (1991) 814.
- [8] R. Gomez, F. Tzompantzi, T. Lopez, O. Navaro, *React. Kinet. Catal. Lett.* 53 (2) (1994) 245.
- [9] S. Damyanova, L. Petrov, M.A. Centeno, P. Grange, *Appl. Catal. A: Gen.* 224 (2002) 271.
- [10] K. Kamiya, S. Sakka, Tatemichi, *J. Mater. Sci.* 15 (1980) 1765.
- [11] J.M. Miller, E.I. Ko, *J. Catal.* 159 (1996) 58.
- [12] W. Beier, A.A. Göktas, G.H. Frischat, *J. Non-Cryst. Sol.* 121 (1990) 163.
- [13] R.G. Rodríguez, J.A. De Los Reyes, J.A. Montoya, T. Viveros, *J. Sol–Gel Sci. Tech.* 33 (2005) 133.
- [14] R.G. Rodríguez Avendaño, J.A. De Los Reyes, J.A. Montoya, T. Viveros, *Superficies y Vacío* 19 (2006) 1.
- [15] J. Ascensión Montoya de la Fuente, *Propiedades estructurales y catalíticas de los sistemas de óxidos metálicos mixtos de Al₂O₃–TiO₂*, Doctoral thesis, UAM-I (1996).
- [16] M. Itoh, H. Hattori, K. Tanabe, *J. Catal.* 35 (1974) 225.
- [17] Ch. Danumah, S.M.J. Zaidi, G. Xu, N. Voyer, S. Giasson, S. Kaliaguine, *Microporous Mater.* 37 (2000) 21.
- [18] J.M. Miller, L.J. Lakshmi, *J. Phys. Chem. B* 102 (1998) 6465.
- [19] S.J. Gregg, K.S.W. Sing, *Adsorption, Surface Area and Porosity*, 2nd ed., Academia Press, London, 1982, p. 195.